CONF-891036--2

CONF-891036--2

DE90 002860

SOLID LUBRICATION OF CERAMIC SURFACES BY IAD-SILVER COATINGS FOR HEAT ENGINE APPLICATIONS

A.Erdemir, G.R. Fenske, F.A. Nichols and R.A. Erck
Tribology Section
Materials and Components Technology Division
Argonne National Laboratory
Argonne IL 60439

For presentation at the 1989 STLE-ASME Tribology Conference
Fort Lauderdale, Florida, October 16-19, 1989

SOLID LUBRICATION OF CERAMIC SURFACES BY IAD-SILVER COATINGS FOR HEAT ENGINE APPLICATIONS.

A. Erdemir, G. R. Fenske, F. A. Nichols and R. A. Erck
Tribology Section
Materials and Components Technology Division
Argonne National Laboratory
Argonne, IL 60439

ABSTRACT

In this study, an investigation was made of the tribological characteristics of alumina ceramics coated with silver by means of ion-assisted deposition (IAD). Tests were performed at temperatures up to 400^{0}C on an oscillating-slider wear test machine capable of simulating the reciprocating motion of a ring/cylinder system. The results showed that higher test temperatures caused greater wear damage and increased friction for uncoated alumina. At 400^{0}C, the wear rates of the alumina-alumina test pairs were 8 to 10 times higher than those tested at room temperature. The steady-state friction coefficients were also fairly high, typically ranging from 0.8 to 1.1. In contrast, the wear rate of IAD-silver coated flats was virtually zero and the wear rates of the counterface pins were reduced by a factor of 72. Friction was also reduced to about half to one third of those for the uncoated pairs. Surface and structure analytical investigations together with the hot-hardness testing of substrate alumina at temperatures up to 600^{0}C were performed to ascertain the mechanisms responsible for the friction and wear behavior of both alumina-alumina and alumina-IAD-silver coated alumina pairs.

INTRODUCTION

The new tribological conditions that have emerged with the advanced heat engine concept call for the development of novel materials and lubricants capable of providing low friction and low wear surfaces at high temperatures under harsh tribological environments [1,2]. Ceramics, owing to their attractive properties at elevated temperatures, are considered as potential candidates for the advanced heat engine applications [3-5]. However, the current state-of-the art in ceramic tribology suggests that without lubrication both the friction coefficients and the wear rates of most ceramics are unacceptably high [6-9], and it is probable that these materials may never be used in heat engines unless new lubricants and/or lubrication concepts are developed.

Recently, the use of directed-ion beams has emerged as a promising practice for achieving improved friction and wear properties on ceramic surfaces. For example, it was observed that ion-assisted deposition (IAD) of silver on alumina and sapphire could markedly improve the wear and friction properties of these ceramics [10]. Unlike other techniques, the IAD process utilizes a high energy ion gun to bombard the surfaces with energetic ions and atoms both prior to and during film deposition. The result is a thin film with better structural density and excellent adhesion to the substrate alumina. Lankford et al. and Wei et al. examined the tribological characteristics of a number of ceramics subjected to high energy ion implantation and ion beam mixing [11,12]. At around 800^0C, certain ion-substrate combinations resulted in low friction and low wear. Hirano and Miyake investigated the effects of high energy ion bombardment on the adhesion, wear and friction properties of Ag and WS_2 coatings [13,14]. They reported significantly improved wear and friction coefficients for coatings prepared by the ion-assisted deposition process. Nastasi et al. evaluated the friction and wear properties of several N-implanted ceramics and concluded that only those ceramics with nitridelike-bond-forming capabilities could provide better tribological performance [15].

In this paper, we deal with the high temperature adhesion, friction and wear characteristics of IAD-silver coatings on alumina ceramics. The selection of silver as the coating material was rather strategic in that, with its low shear strength, high thermal conductivity, excellent chemical inertness and moderately high melting point, we felt that it could help in reducing not only the frictional losses but also the severe wear damage in ceramics. In general, ceramic materials are known to be very brittle, insulating and somewhat sensitive to the service environments. Furthermore, silver has long been used in various tribological applications including the PS-200 composite coatings that possess excellent tribological properties at high temperatures [16].

EXPERIMENTAL DETAILS

Test Materials

The flat alumina specimens were obtained from commercial sources with standard dimensions of 38.1 x 50.8 x 4.2 mm, an average surface roughness of about 0.3 m CLA and grain sizes ranging from 10 to 20 m. To avoid surface damage which may occur during mechanical grinding and polishing [17], the flat samples were tested in as-sintered conditions. 9.52 mm diameter alumina balls with a surface finish of approximately 0.03 m CLA were used as the pin counterparts. Alumina balls were firmly secured on a special holder to make up the stationary pin specimens of the pin-on-flat configuration. All specimens were ultrasonically cleaned sequentially in trichlorethylene, acetone and methanol for 10 minutes each, then dried in an oven at 110°C for 20 minutes.

The IAD-silver films were prepared in a high vacuum chamber incorporating an electron beam evaporator and an ion beam gun. The details of this deposition process and the procedures followed in this study can be found in a recent paper by these authors [10].

Friction, Wear and Hot-hardness Tests

The friction and wear tests were conducted on an oscillating-slider test apparatus that provided a sliding motion similar to that between a piston ring and a cylinder in an operating engine. As can be visualized from the schematic in Figure 1, the pin specimen was drawn back and forth across the stationary flat. The frequency and the stroke length were 1 Hz and 25 mm respectively. Each test was run for a total of 1000 cycles. The dead weight on top of the pin specimen sliding against the flat was 10 N which created a mean Hertzian pressure of about 0.84 GPa. The room humidity varied between 16 and 20% during the tests. Tests were ran at 23, 200 and

400^0C. The friction force was monitored by means of a strain gauge transducer and recorded continuously throughout the tests. The wear volume measurement on pin specimens was based on the microscopic determination of the wear scar diameters which were subsequently converted into wear volume by a mathematical formula suggested by Fischer et al. [18]. The wear of flat specimens was assessed from the traces of surface profile across the wear tracks. For better reliability and reproducibility, a total of three duplicate tests were run at each temperature and the mean average was taken to represent the friction and wear data.

For the higher temperature friction and wear tests, a series of electrical cartridge heaters were inserted into the top and the bottom stainless steel plates that housed the pin and flat specimens. The test zone was allowed to first reach then and stabilize at these temperatures for a duration of 800 seconds. The wear tracks and the scars as well as the wear debris particles were examined on a scanning electron microscope equipped with an energy dispersive X-ray analyzer. To overcome charging, a thin carbon film (about 12 nm thick) was sputter-deposited on the surfaces.

In correlating hardness to wear properties, it is important that the measurements be made at identical temperatures. Therefore, the hardness measurements were performed on uncoated alumina samples by utilizing a commercial unit at room temperature, 200, 400 and 600^0C, and under a load of 500 g. and in a vacuum environment with a base pressure of 10^{-5} Torr. The Vickers diamond indenter and the specimen stage were independently heated up to these temperatures and stabilized for 5 to 7 minutes before taking a measurement. For better microscopic view and smoother indentation, the samples were diamond polished to a surface finish of about 0.05 CLA. Measurements were taken during both the heating-up and the cooling down cycles. At least three measurements were made at each temperature and the mean average was taken as the representative data point.

RESULTS

Friction

The friction coefficients for all the test pairs are presented in Figure 2. In general, all the alumina/alumina test pairs exhibit high friction coefficients ranging from 0.8 to 1.1. Note that the pairs tested at room temperature, exhibit an initial friction coefficient of about 0.8 which sharply increases to 0.95 before stabilizing at around 0.85. In contrast, the friction coefficients of the pairs tested at 200 and 400^{0}C start at higher values of 0.93 and 1 respectively, and remain around these values for the duration of wear tests.

The pairs with a silver film show significantly lower friction coefficients. When tested at room temperature, their initial friction coefficients are about 0.17 which increases gradually with distance and stabilizes at a value of around 0.6. The friction coefficients of the pairs tested at 200 and 400^{0}C are initially 0.3. In the later stages of the sliding, these pairs exhibit fairly modest increases in their friction coefficients with distance before reaching a steady-state regime.

Wear and Hot-hardness

Table 1 summarizes the results of both wear and hot-hardness measurements on alumina specimens as a function of ambient temperature.

Table 1. Wear rates and Vickers hardness of uncoated Al_2O_3 and IAD-Ag coated Al_2O_3 specimens as a function of test temperatures.

Test Materials Pin	Disc	Temperature (C)	Pin Wear Rate (10^{-7} mm^3/N.m)	Disc Wear Rate (10^{-6} mm^3/N.m)	$VHN_{0.5Kg}$ (Kg/mm^2)
Al_2O_3	Al_2O_3	23	247	283	1752
		200	1035	626	1405
		400	2040	875	1102
		600	-	-	821
Al_2O_3	Ag-coated Al_2O_3	23	62	immeasurable	-
		200	40	immeasurable	-
		400	28	immeasurable	-

The wear data in Table 1 suggest that increasing temperature (1) significantly lowers the hardness of alumina substrates, and (2) dramatically increases the wear rates of both the pins and the flats. For example, the wear rate of the pins sliding against the flats increases by a factor of 9 when tested at 400^{0}C. Note that the wear rate and the hardness of alumina appear to be inversely related to each other within the temperature range evaluated, hence suggesting that the Archard's wear law is obeyed.

In contrast, for the pairs comprising an IAD-silver coating, the wear rates of the pins were smaller than for the pairs without a silver film by a factor of about 4 at room temperature, and by about 70 at 400^{0}C. More interestingly, the wear of silver coated alumina flats was essentially zero, hence making it very difficult to measure by the surface profilometry technique used in this study.

Wear Surface Analyses

A series of electron micrographs shown in Figures 3 through 5 display the typical features of all the worn surfaces. Low magnification images in Figure 3 reveals two distinct features; one relates to microfracture and the other is evidence of some macroscale plastic deformation. While the cracks with intergranular and transgranular fracture patterns were more dominant on surfaces worn at room temperature, the wear tracks of the samples tested at 200 and 400^{0}C, contained some smooth plateaus which appeared to be plastically deformed (see Figure 3b and c). The degree of plastic flow appeared to be more pronounced in specimens tested at 400^{0}C than at 200^{0}C.

However at much higher magnifications, it become clear that those plateaus with plastic flow patterns were in fact made up of densely -packed wear debris particles whose sizes ranged from 10 to 100 nm (see Fig. 4). The micrographs in Figure 5 show the other outstanding features of all the worn surfaces. These include grain boundary sliding in Figure 5a, highly crystallographic fracture pattern in Figure 5b, and cleavage crack initiating from volume defects in and around the grains in Fig. 5c.

Insofar as the silver-coated test specimens are concerned, a closer examination of their wear tracks indicates that silver films remained largely intact on the surfaces during the entire course of sliding, but underwent heavy shear deformation to accommodate the normal as well as the tangential forces generated during the dynamic action of oscillating sliding (see Figures 6a, b and c). In short, the substrate alumina appears to be well-protected by the IAD-silver coatings and the wear of the underlying substrates is very difficult to assess. A higher magnification electron micrograph in Figures 6c reveals that only the summits of the surface asperities (distinguished with dark spots in the micrographs) of alumina were exposed and slightly worn away (denoted by an arrow). The silver film itself appeared to fill in the valleys between these asperities to provide better load bearing capacity and/or cushioning.

The energy disperive x-ray analyses revealed that regardless of the test temperatures, some silver was always transferred onto the wear scars of the pin specimens (see Figure 7). This type of transfer film behavior is of importance in practical applications, since such transfer from one face to another will retain the lubricous film material within the contact zone, hence reducing the need for periodic resupply. One adverse effect of such behavior is that the formation and subsequent rupture of the micro-junctions between the parent and transferred films may increase the overall friction coefficient.

Wear Debris Analysis

The micrographs in Figure 8 display the size, shape and fracture morphology of the wear debris particles recovered from the wear surfaces. Note that what appeared to be lumps or large wear fragments in the magnification micrographs were revealed at higher magnification to be heavily compacted and sintered submicron-size wear debris particles. The degree of sintering appeared to be significantly greater at higher test temperatures.

DISCUSSION

Friction

Al_2O_3/Al_2O_3 Test Pairs

The somewhat lower initial and steady-state friction coefficients of the pairs tested at room temperature (see Fig.2) can be attributed to the precipitation of an adsorbed film on the surfaces from the test environment [18,19]. The occurrence of a steep increase with increasing distance confirms the above hypothesis by indicating that the adsorbed film was rapidly being removed from the contact zone and the establishment of better ceramic-to-ceramic contact was in progress.

The higher friction coefficients at elevated temperatures can be attributed to a number of phenomena. First of all, the adsorbed layer which acted as a lubricant at room temperature is probably absent. Second, a higher degree of thermal excitation is present for increased atomic interaction and/or adhesion. Finally, owing to a significantly larger contact area, both the plowing and adhesion terms of the total friction are significantly increased at these higher temperatures. Overall, the range of friction coefficients for alumina pairs reported here, is fairly consistent with the existing data reported elsewhere [3,20].

Al_2O_3/Silver-Coated Al_2O_3

We believe that two factors critically influence the frictional behavior of pairs which include an IAD-silver coating: namely the high adhesion and the low shear strength of silver film. First of all, it is known that the film-to-substrate adhesion is of utmost importance for achieving not only longer wear life but also lower friction. In a recent study, these authors demonstrated that silver films without adequate adhesion (i.e., PVD-Ag films) would fail rapidly under tribological loading and lead to a severe case of ceramic-to-ceramic contact which in turn triggered heavy wear damage and high frictional losses [10]. The results of this study further demonstrated that the IAD-silver films are capable of reducing both the wear rates and the friction coefficients of alumina ceramics not only at room temperature but also at fairly elevated temperatures. Even though we do not have any quantitative data pertaining to the adhesive strength of the IAD-silver coatings dealt with in this study, these coatings have proven themselves to be adherent enough to endure both the normal and tangential components of the surface contact stresses which were rather severe and reversed direction once per second.

Generally low friction of the pairs comprising a silver film, is largely due to the low shear strength of silver. Shear bands (see Fig. 6) with preferred alignment strongly suggests that silver indeed undergoes heavy shear deformation during sliding to reduce the tangential stresses, hence the friction.

In specific, It is known that in addition to shear strength, there are several intrinsic as well as extrinsic parameters play active roles in the overall frictional behavior of most solid lubricants. Some of these include load, speed, environment, surface roughness and coating thickness [21]. Moreover, silver is known to provide low friction against some materials, like steel, but quite high friction when slid against others, like nickel. Peterson attributes this type of disparity to the extent of miscibility between silver and these materials [22]. The higher the extent of miscibility, the greater is the friction coefficient. The extent of the solubility of Ag in Al_2O_3 is not known at present. However, Peiffer reported that the composite alloys made from Ag and Al_2O_3 were quite capable of exhibiting strength and resistance to adhesive failure at temperatures above the melting point of the silver [23]. In addition, the presence of a transfer film on the rubbing surfaces of all the pins slid against the silver coated flats (see Fig. 7) suggests that there may indeed exist some form of interaction between silver and alumina. Hence, in keeping with the adhesion theory of friction, somewhat high friction coefficients reported in Figure 2 can be attributed to the formation and subsequent rupture of junctions between silver and transferred silver as well as silver and alumina.

Figure 2 showed that pairs tested at elevated temperatures generally exhibited lower friction coefficients than the pairs tested at room temperature. We attribute this trend to the thermal softening of silver, making it even more shearable and/or less viscous.

Wear

Al_2O_3/Al_2O_3 Pairs:

An overview of the models proposed for the wear behavior of ceramics suggests that deformation [24], microfracture [18,25], thermomechanical [26] and tribochemical [18,19] interactions may take place in a given tribosystem and generate wear. Under the conditions explored in this study, the hardness data in Table 1 suggest that plastic deformation is one of the mechanisms by which the alumina surface wears. Furthermore, microscopic evidence in Figures 3-5 suggests that microfracture is the other dominant mechanism of wear. Wear due to tribochemical and thermomechanical interactions can not be ruled out, but the physical evidence for these types of wear are lacking, and the sliding velocity and the test environment were not at levels high enough to trigger these types of wear. Therefore, we believe that under the test conditions of this study, wear occurred largely by microfracture and to some extent by deformation. This is further rationalized by the following arguments.

Based on the inverse relationship between the wear rate and the hot-hardness data in Table 1, one might conclude that wear was predominantly controlled by a mechanism involving heavy plastic deformation and the Archard's wear law was largely obeyed. However, even the micro-scale features of the worn surfaces contradicts this view by revealing large scale brittle fracture (see Fig. 3-5). The existence of some grain boundary sliding in Figure 5a was an indication of some plastic deformation, especially at higher test temperatures, but other than that, there was no microscopic evidence indicative of plastic deformation. What appeared at low magnification to be macro-scale plastic deformation (see Fig. 3), turned out on closer inspections, to be large islands of compacted and/or sintered fine wear particles (see Fig. 4). Even though the presence of subsurface deformation due to dislocation and twinning can not be ruled out, nevertheless, electron microscopic examination failed to support the hardness data which suggested a wear mechanism related to gross-plastic deformation.

According to the fracture mechanical studies, alumina, owing to its partially covalent atomic bonds and highly anisotropic crystal structure, hardly deforms plastically at room temperature in considerable amounts. The yield and fracture strengths are reported to be almost identical when tested in tension [27]. However, under highly localized compression, like diamond indentation it was shown to undergo some micro-scale plastic deformation even at room temperature [28]. Based on the scanning electron microscopic evidence only, we can say that under the conditions of our sliding tests, microfracture was the principal mechanism for the wear of alumina. Highly concentrated loading and unloading of a surface through a pin in normal directions are known to create large tensile and compressive stresses in tangential directions. Such stresses in turn (1) weaken the grain boundaries and eventually may lead to grain pullouts (see Fig. 5a), (2) can initiate microcracks at voids and other imperfections (see Fig. 5a and b), and (3) cause cleavage cracks with preferred crystallographic orientations (see Fig. 5c). Wear fragments produced in this manner become trapped between the sliding surfaces where they undergo severe mechanical grinding to make-up those very fine wear debris particles whose sizes ranged from 10 to 100 nm (see Fig. 8). While some debris particles remain loose on the surface, some are heavily compacted and/or sintered to make-up the islands seen in Figure 3. The formation of similar types of debris particles and islands was observed on other ceramics even under lubricated test conditions [19].

Al_2O_3/Ag-coated Al_2O_3

The superior wear performance of pairs including a silver film can be attributed to the excellent adhesion of the coatings which effectively prevented direct ceramic-to-ceramic contacts. Moreover, owing to its low shear strength, silver as a surface film (1) increases the load bearing capacity of underlying substrate ceramics via cushioning, (2) reduces the detrimental effects of compressive and tensile stresses generated at the leading and trailing edges of the oscillating pin, and (3) displaces the location of maximum ortagonal shear stress away from the surface, hence reducing the probability of surface initiated cracks. Despite its adverse effect on friction, the transferred silver film on counterface material (see Fig. 7) can be regarded as beneficial against wear, in particular against the wear of counterface pins.

CONCLUSIONS

Based on the experimental results reported above, the following conclusions can be drawn:

(1) Under the test conditions of this study, the unlubricated sliding of alumina test pairs on themselves causes high friction and wear losses. Increasing ambient temperature has a detrimental

effect on the wear behavior of alumina.

(2) The hardness of alumina decreases significantly with increasing temperature and inversely relates to the wear rate. Microfracture together with deformation are the major mechanisms for the wear of alumina ceramics. Sub-micron size particles are the dominant wear debris particles produced on the rubbing surfaces. They are generally trapped and densely compacted between rubbing surfaces and appeared as large wear plateaus.

(3) Owing to its good adhesion and easy shear capability, silver film produced by the IAD process can virtually eliminate the wear of flats and markedly reduce the wear of counterface pins rubbing against these silver-coated flats. Further, thin silver films can significantly reduce the friction coefficients of alumina ceramics. The beneficial effect of silver becomes even more pronounced at higher test temperatures.

(4) In selecting these and other ceramic materials for heat engine applications, it is important that the degenerative actions of both microfracture and deformation should be recognized as serious problems, especially in regions near the top- and bottom-dead centers where the sliding speed is low and the frictional traction is high (as in our case). Surface modification of ceramics by technologies utilizing energetic ions may be considered as viable alternatives for reducing the friction and wear losses in actual engine environments.

ACKNOWLEDGEMENT

Work sponsored by the Tribology Program, U.S. Department of Energy, Energy Conversion and Utilization Technologies Division, Office of Energy Utilization Research.

REFERENCES

1. Kanakia, M., Owens, M. E., and Ling, F. F., "Solid Lubrication of Advanced Heat Engines", in Proceedings of Workshop on Fundamentals of High Temperature Friction and Wear with Emphasis on Solid Lubrication for Heat Engines", ed by F. F. Ling, Troy, NY (1984), p. 19.

2. "Tribology of Ceramics", National Materials Advisory Board, National Academy Press, 1988, NMAB Publication #435.

3. Cranmaer, D. C., "Ceramic Tribology, Needs and Opportunities", Tribologgy Transactions, 31(1988), p. 164.

4. Mehrotra, P. K., "Evaluation of Engineering Ceramics for Wear Applications", ASME, Wear of Ceramics, p. 301

5. Breznak, J., Breval, E., and Macmillan, N. H., "Sliding Friction and Wear of Structural Ceramics", J. Mater. Sci., 20(1985) p.4657

6. Sutor, P., "Tribology of Silicon Nitride and Silicon Nitride-Steel Sliding Pairs", Ceram. Eng. Sci. Proc., 5(1984), 460-469.

7. Dufrane, K. F., and Glaeser, W. A., "Wear of Ceramics in Advanced Heat Engine Applications", ASME, Wear of Materials, 1987, p. 285

8. Sikra, J. C., Krysiak J. E., and Ruh, R., "Friction and Wear Characteristics of Selected Ceramics", Am. Ceram. Soc. Bulletin, 53(1974), 581

9. Dufrane, K. F., "Wear Performance of Ceramics in Ring/Cylinder Applications", Ceram. Eng. Sci. Proc., 9(1988) 1409-1418.

10. Erdemir, A, Fenske, G. R., Erck R. E., and Cheng, C. C.,"Ion-Assisted Deposition of Silver Films on Ceramics for Friction and Wear Control", To be published in Lubric. Eng., 1989

11. Lankford, J., Wei W., and Kossowsky, R., "Friction and Wear Behavior of Ion-beam-modified Ceramics", J. Mater. Sci., 22(1987), 2069-2078.

12. Wei, W., Lankford J., and Kossowsky, R., "Friction and Wear of Ion-beam-modified Ceramics for Use in High Temperature Adiabatic Engines", Mat. Sci. Eng. 90(1987) 307-315

13. Hirano, M., and Miyake, S., "Effect of High Energy Ion Bombardment on the Tribological Properties of WS_2 Sputtered Films", J. Trib., 110(1988), 621-627.

14. Hirano, M., and Miyake, S., "Tribological Improvement of Ag Films by Ion Beam Enhanced Deposition," ASME J. Trib., 110(1988),p.

15. Nastasi, M., Kossowsky, R., Hirvonen, J. P., and Elliott, N., "Friction and Wear Studies in N-Implanted Al_2O_3, SiC, TiB_2 and B_4C Ceramics, J. Mater, Res. 3(1988), p. 1127-1133.

16. DellaCorte, C., Sliney H. E., and Deadmore, D. L., "Sputtered Silver Films to Improve Chromium Carbide Based Solid Lubricant Coatings for Use to 900 C.", STLE Trans., 31, 3, 1988, p. 329

17. Swain, M. V., "Microscopic Observation of Abrasive Wear of Polycrystalline Alumina", Wear, 35(1975), pp. 185-189

18. Fischer, T. E., and Tomizawa, H., "Interaction of Tribochemistry and Microfracture in the Friction and Wear of Silicon Nitride", Wear of Materials, ASME, (1985) p. 22

19. Jahanmir, S and Fischer, T. E., "Friction and Wear of Silicon Nitride Lubricated by Humid Air, Water, Hexadecane and Hexadecane+0.5 Percent Stearic Acid", STLE Trans. 31(1988) p.32-43.

20. Wallbridge, N., Dowson, D., and Roberts, E. W., "The Wear Characteristics of Sliding Pairs of High Density Polycrystalline Aluminum Oxide Under Both Dry and Wet Conditions", Wear of Materials, 1983, K. C. Ludema, ed., ASME, New York, pp 202-211 (1983)

21. Sherbiney, M. A., and Halling, J., "Friction and Wear of Ion-Plated Soft Metallic Films", Wear, 45(1977), pp 211-220

22. Peterson, M. B., Private Communication, Argonne National Laboratory, February 1989.

23. Peiffer, H. R., "The Behavior of Composite Silver-Alumina Alloys Above the Melting Point of Silver", Trans. Met., AIME., 218(1960) pp. 775-777

24. Ajayi, O. O., and Ludema, K. C., "Surface Damage of Structural Ceramics: Implications for Wear Modelling, Wear of Materials, 1987, K. C. Ludema, ed., ASME, New York, pp. 349-360, (1987).

25. Buckley, D. H., and Miyoshi, K., "Friction and Wear of Ceramics", Wear, 100(1984), pp. 333-353

26. Winer, W. O., and Ting, B. Y., "Development of a Theory of Wear of Ceramics", Final Report to Oak Ridge National Laboratory, ORNL/84-7802/1, Oak Ridge, TN, 1988

27. Terwilliger, G. R., and Redford, R., "High Temperature Deformation of Ceramics: Specific Behavior," Am. Ceram. Soc. Bull., 53(1974), pp. 465-472

28. Hockey, B. J., "Plastic Deformation of Aluminum Oxide by

Indentation and Abrasion," J. Am. Ceram. Soc., 54(1971), p. 223.

FIGURE CAPTIONS:

Figure 1. A schematic representation of the oscillating-slider wear test machine.

Figure 2. Variation of friction coefficients of alumina-alumina and alumina-IAD-silver coated alumina test pairs with sliding distance and ambient temperature.

Figure 3. SEM micrographs of wear tracks on flat alumina specimens after testing at a) room temperature, b) 200^0, and c) 400^0C.

Figure 4. High magnification SEM micrographs of the plateaus seen on the wear tracks formed at a) room temperature, b) 200^0, and c) 400^0C.

Figure 5. SEM micrographs of a) brittle fracture and grain boundary sliding, b) highly crystallographic cleavage fracture, and c) cracks initiating from a void.

Figure 6. SEM micrographs of the typical wear tracks formed on IAD-silver coated alumina flats; a) secondary-electron image, b) back-scattered electron image, and c) high magnification secondary-electron image.

Figure 7. a) An SEM micrograph, and b) an Ag-x-ray map of a wear scar formed on an alumina pin while sliding against an alumina disc coated with IAD-silver.

Figure 8. SEM micrographs of the alumina wear-debris-particles formed at 200^0C; a) low magnification, and b) high magnification images.

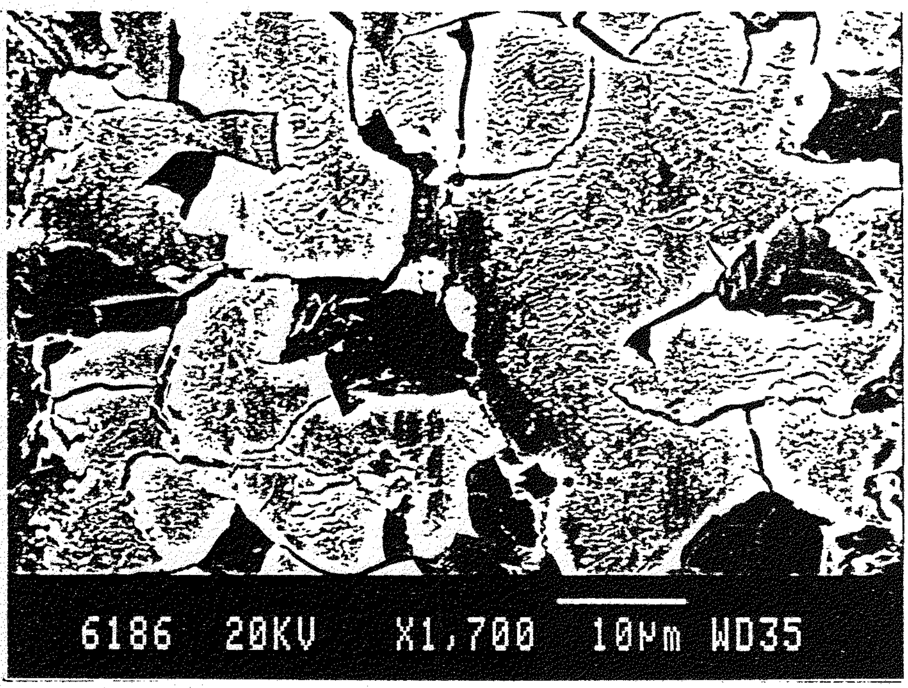

(a)

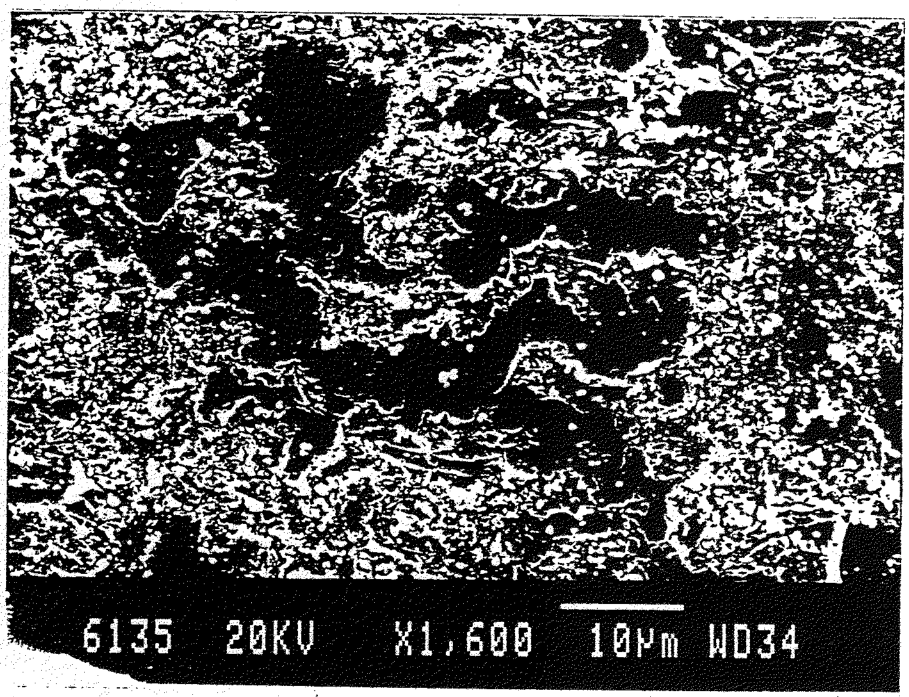

(b)

Fig.3

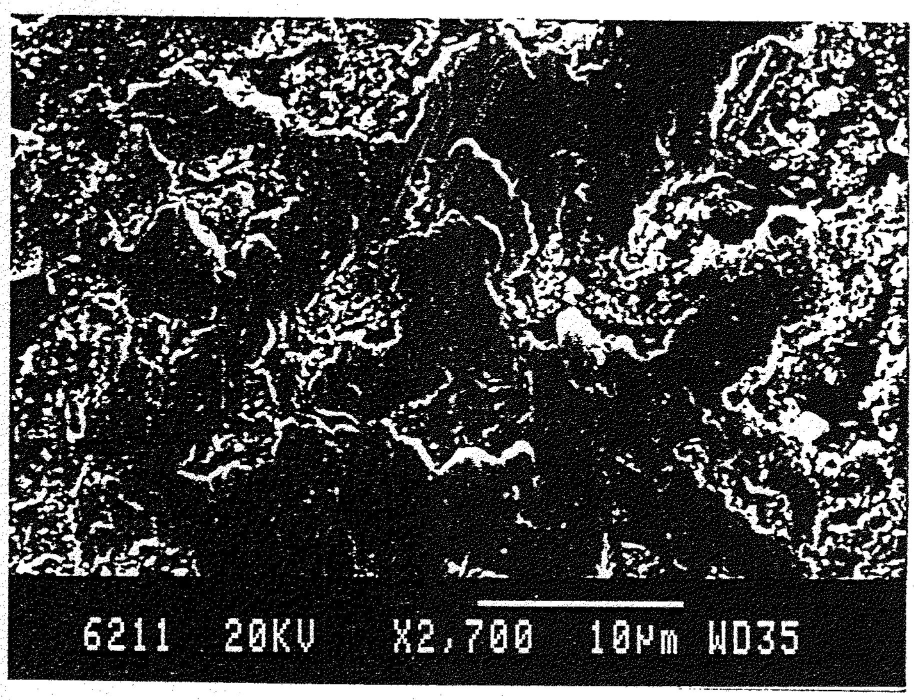

(c)

Fig.3

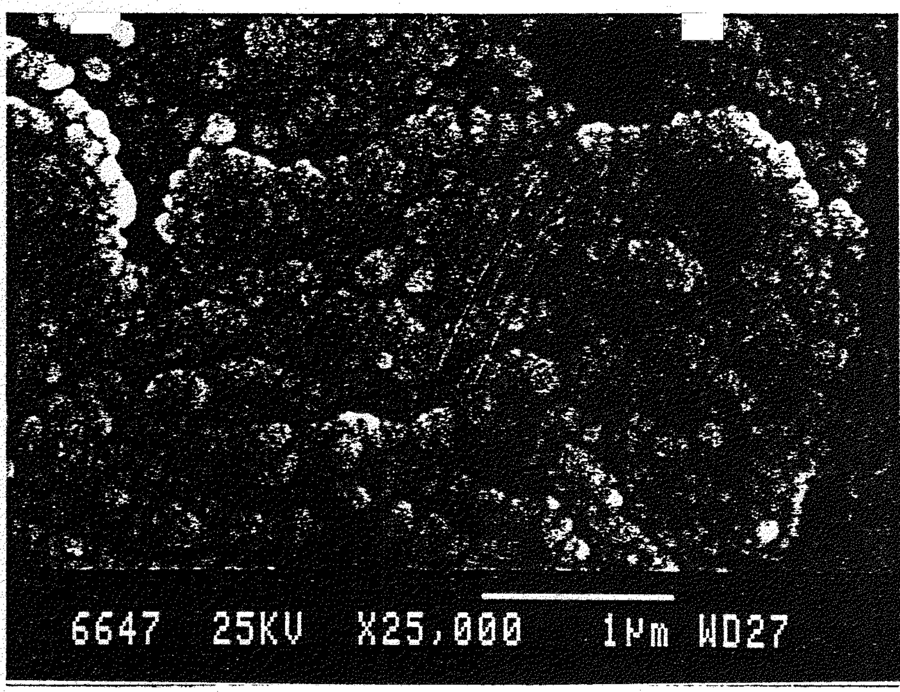

(a)

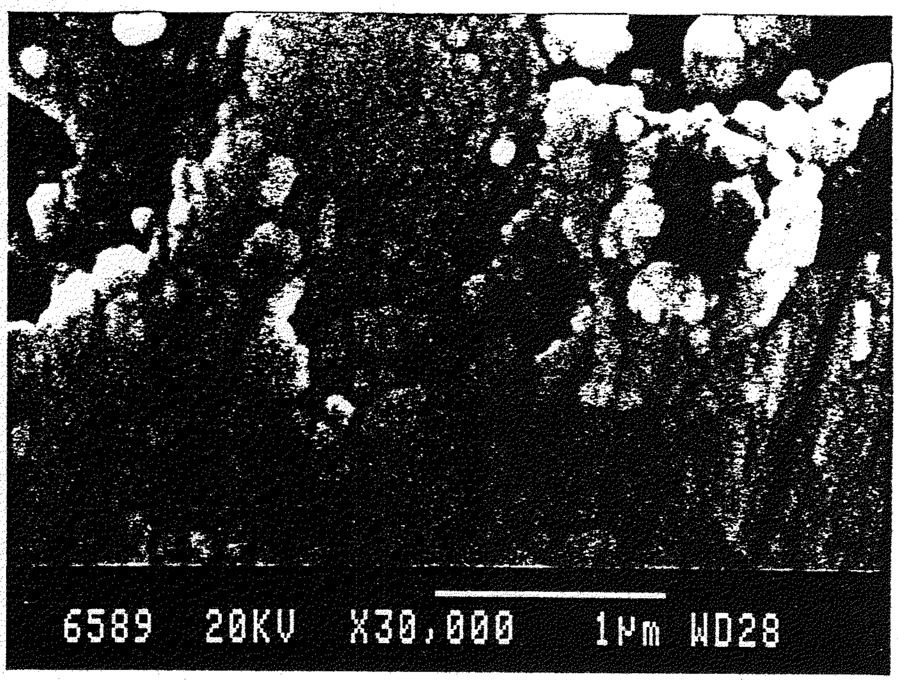

(b)

Fig. 4

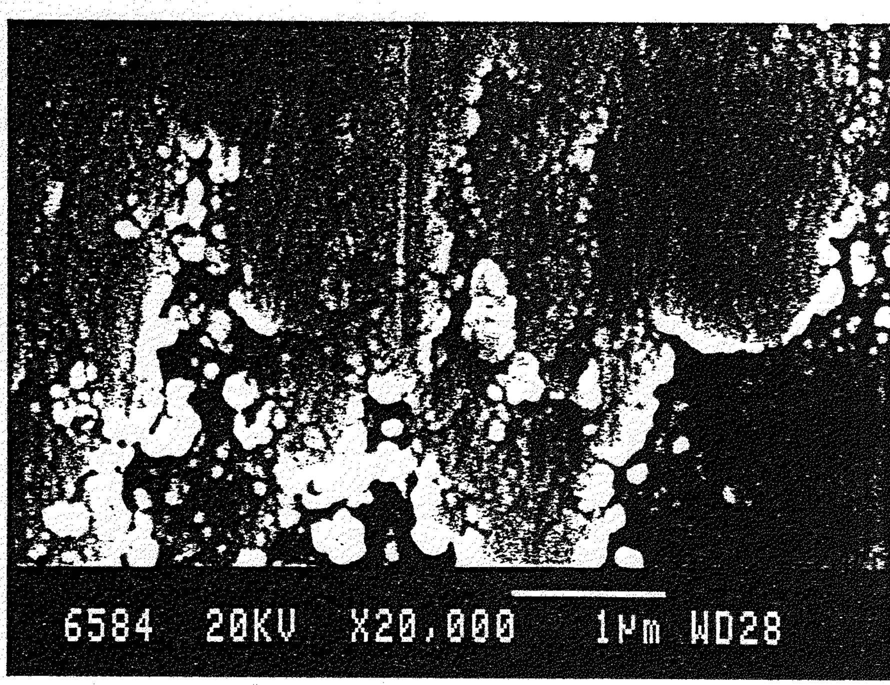

(c)

Fig.4

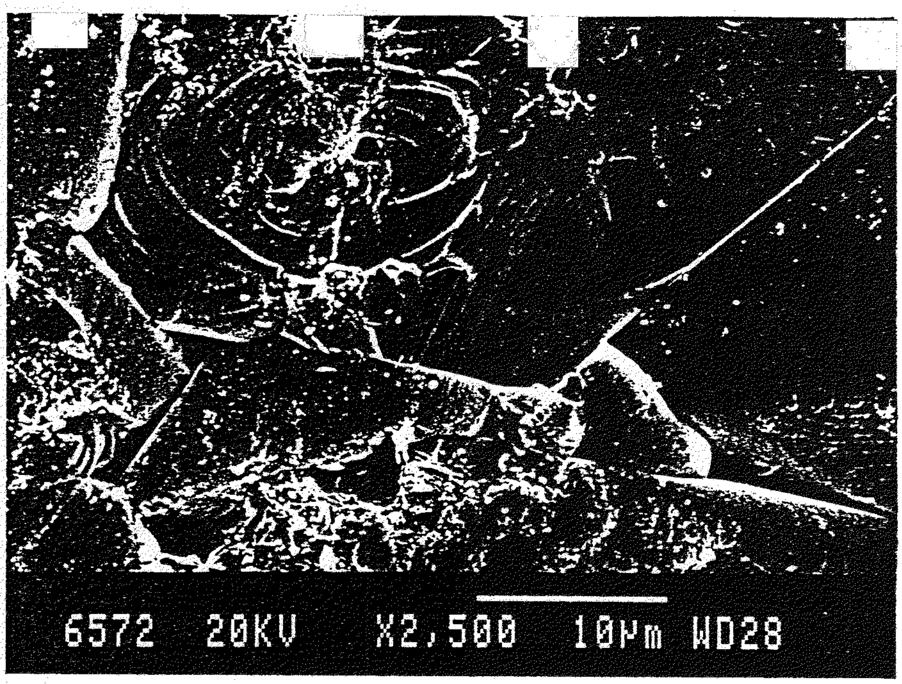

(a)

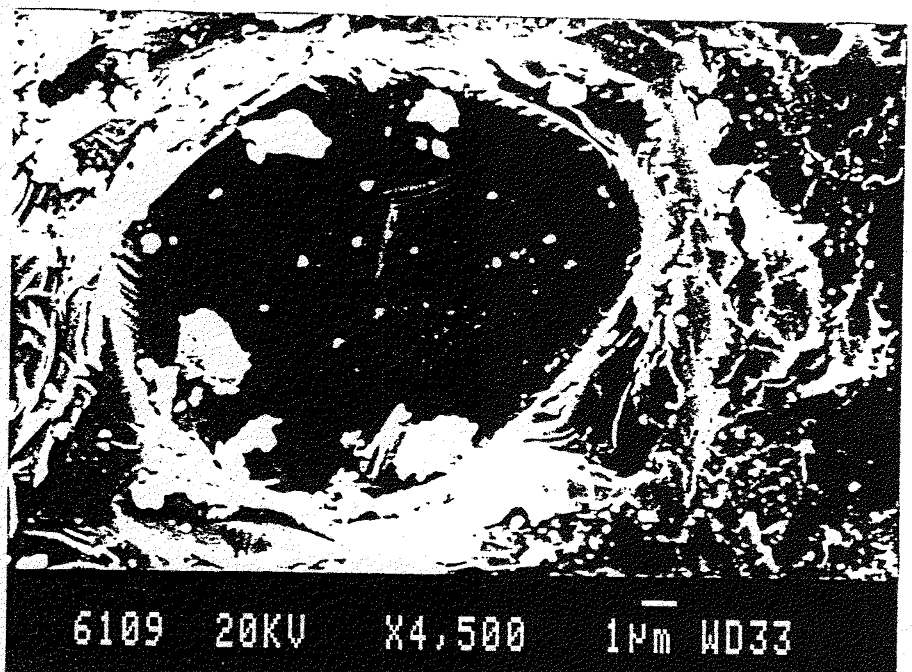

(b)
Fig.5

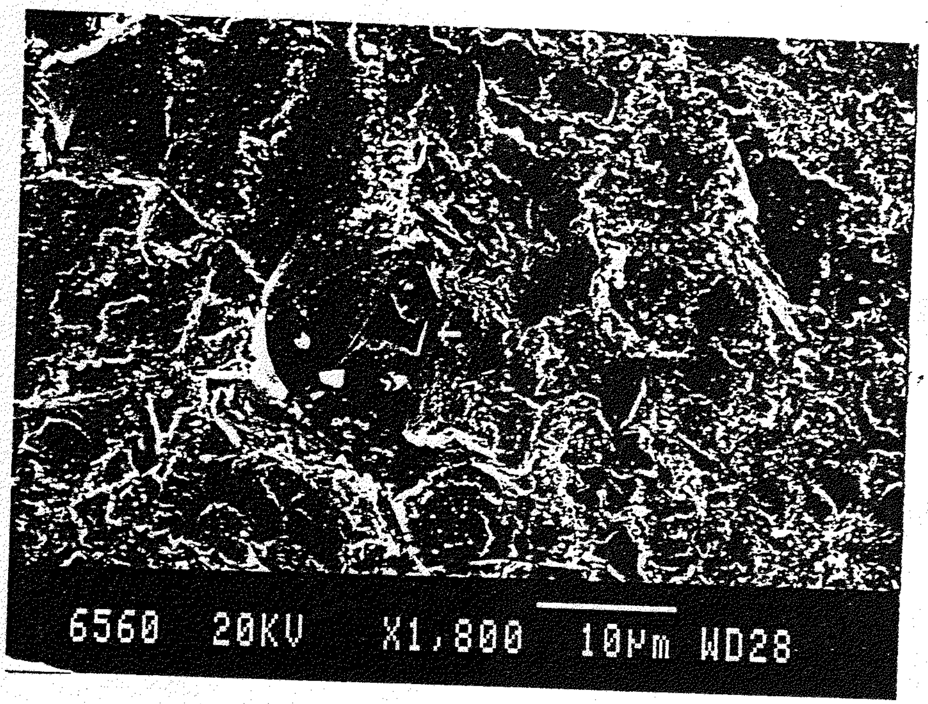

(c)

Fig.5

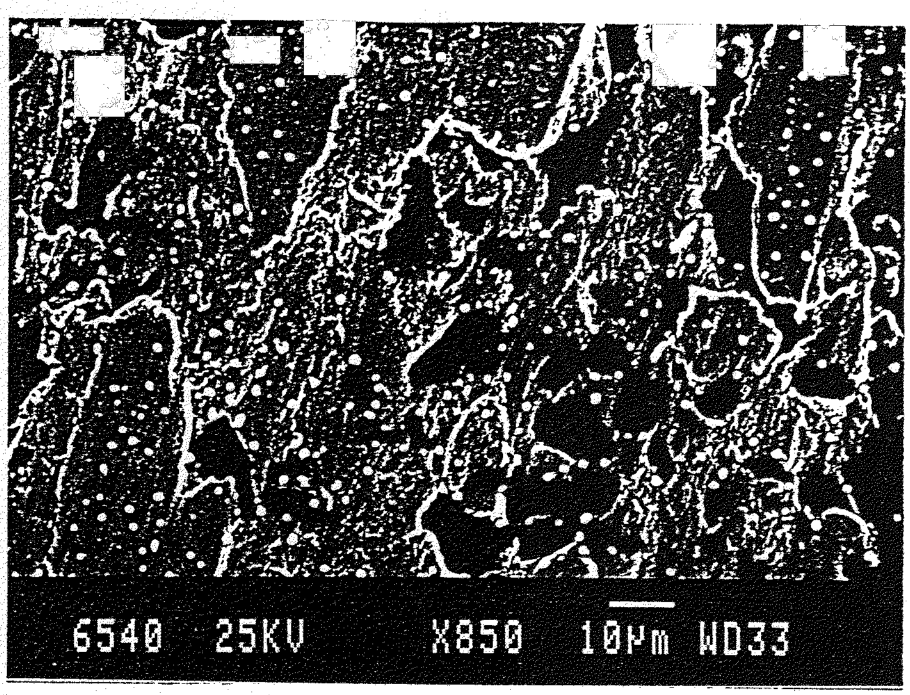

(a)

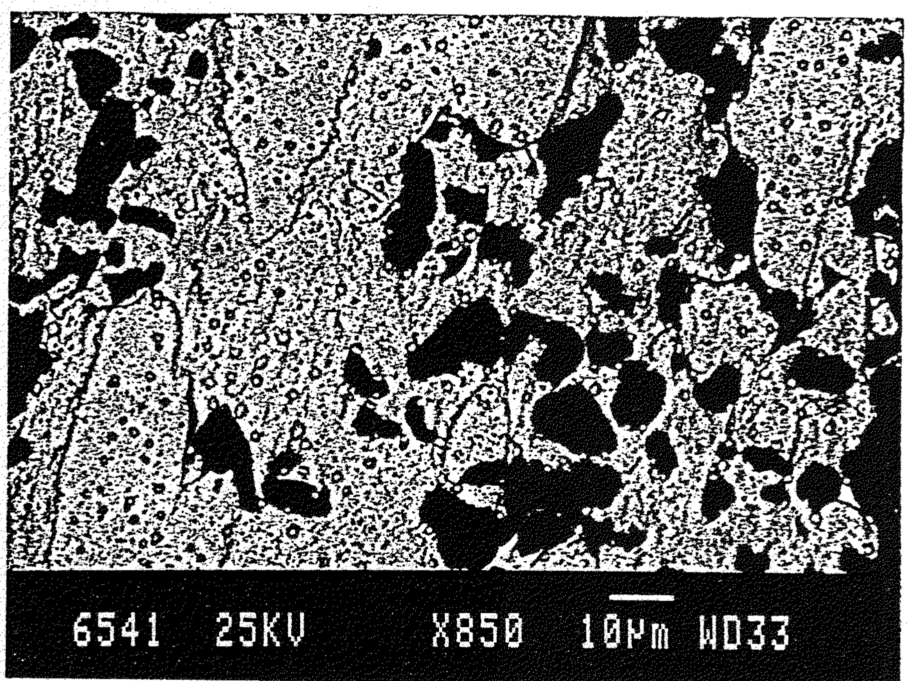

(b)
Fig. 6

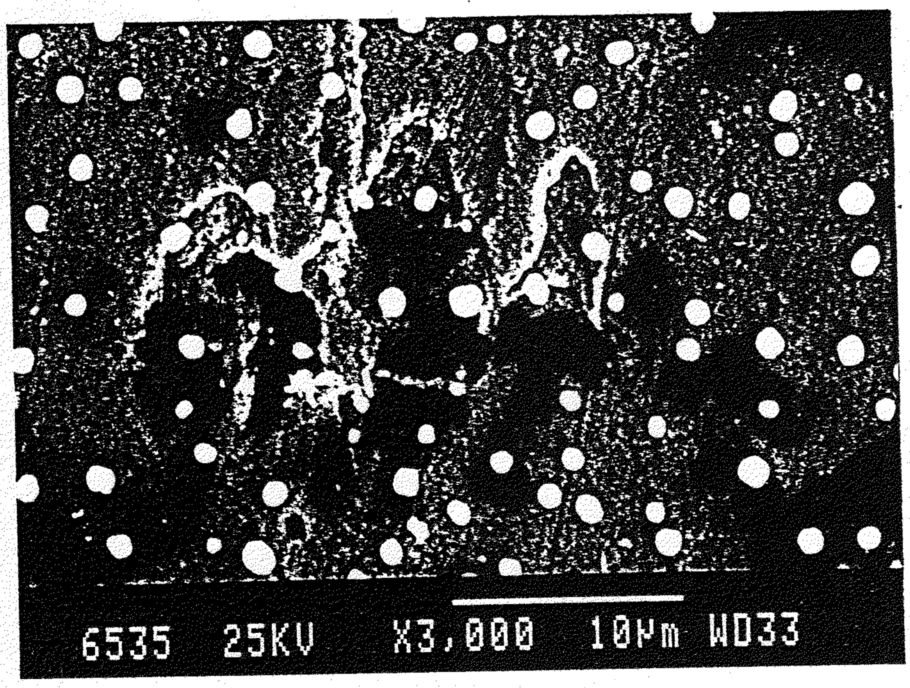

(c)

Fig. 6

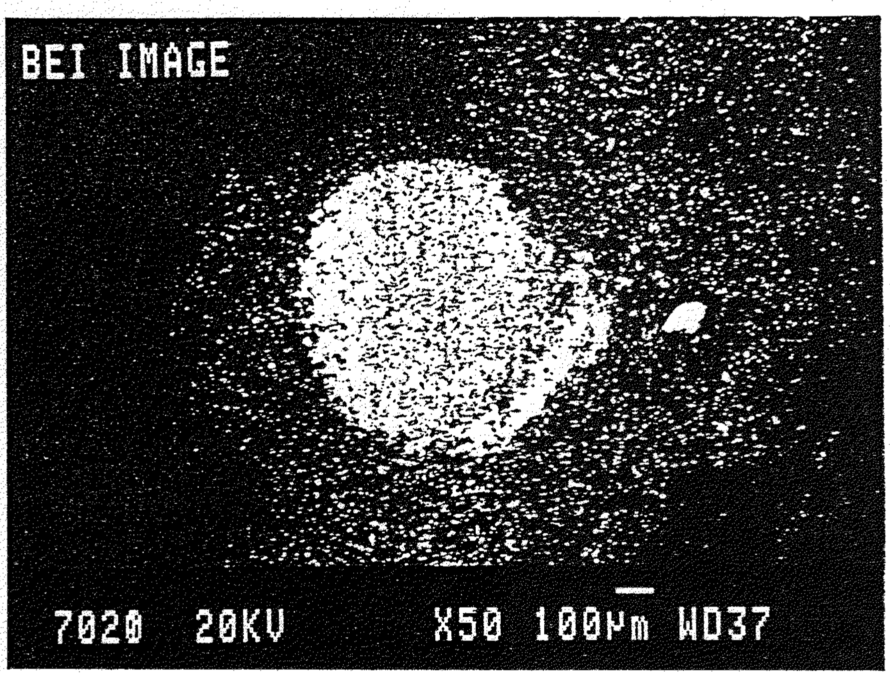
BEI IMAGE
7020 20KV X50 100μm WD37

(a)

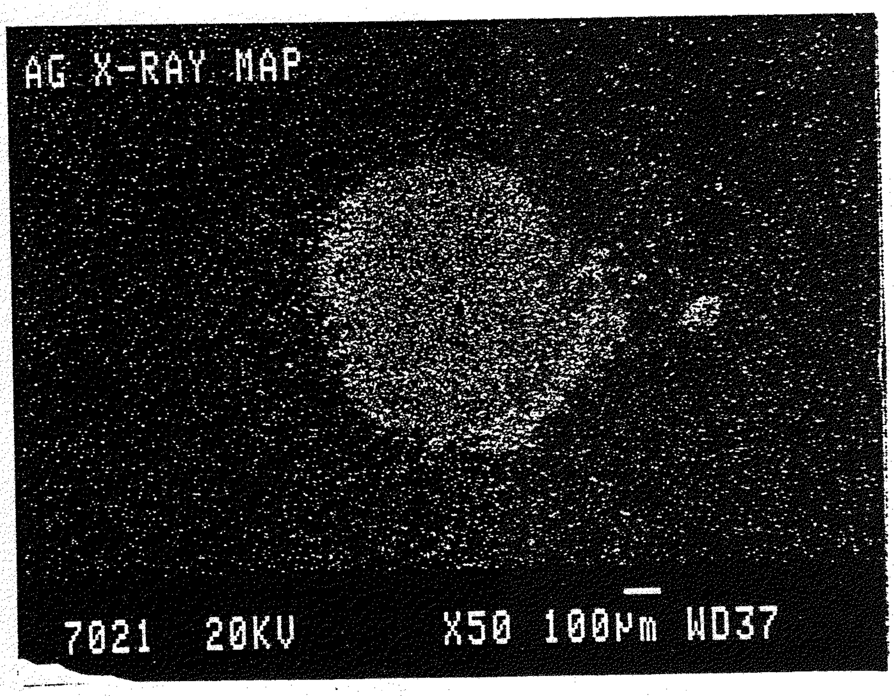
AG X-RAY MAP
7021 20KV X50 100μm WD37

(b)
Fig. 7

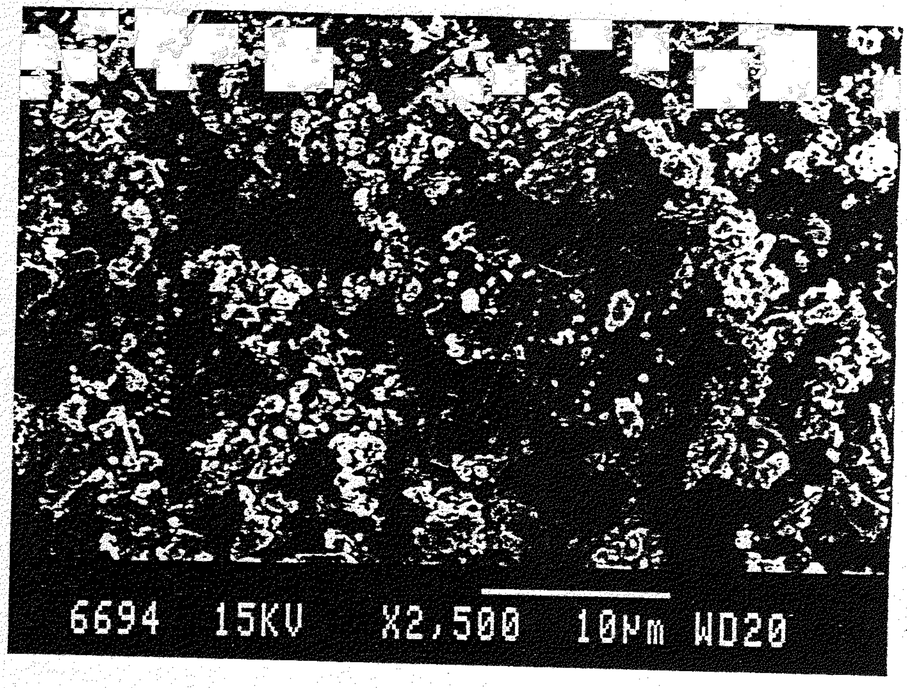

(a)

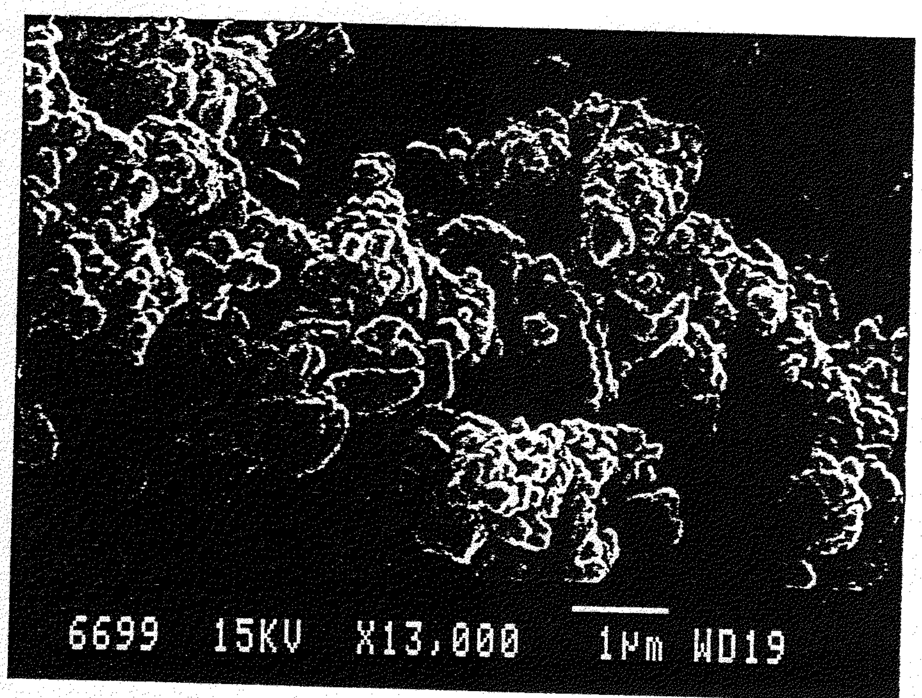

(b)
Fig. 8